Journal of Medical Engineering & Technology, Vol. 32, No. 2, March/April 2008, 103–114

informa
healthcare

Advanced integrated technique in breast cancer thermography

E. Y. K. NG*† and E. C. KEE‡

†School of Mechanical and Aerospace Engineering, College of Engineering, Nanyang Technological University, 639798, Singapore
‡Goodrich Aerostructures, 41 Changi North Crescent, 499638, Singapore

(*Received 31 October 2005; in final form 28 December 2005*)

Thermography is a passive and non-contact imaging technique used extensively in the medical arena, but in relation to breast care, it has not been accepted as being on a par with mammography. This paper proposes the analysis of thermograms with the use of artificial neural networks (ANN) and bio-statistical methods, including regression and receiver operating characteristics (ROC). It is desired that through these approaches, highly accurate diagnosis using thermography techniques can be achieved. The suggested method is a multi-pronged approach comprising of linear regression, radial basis function network (RBFN) and ROC analysis. It is a novel, integrative and powerful technique that can be used to analyse large amounts of complicated measured data such as temperature values extracted from abnormal and healthy breast thermograms. The use of regression allows the correlation between the variables and the actual health status of the subject, which is decided by other traditional means such as the gold standard of mammography for breast cancer detection. This is important as it helps to select the appropriate variables to be used as inputs for building the neural network. RBFN is next trained to produce the desired outcome that is either positive or negative. When this is done, the RBFN possess the ability to predict the outcome when there are new input variables. The advantages of using RBFN include fast training of superior classification and decision-making abilities as compared to other networks such as backpropagation. Lastly, ROC is applied to evaluate the sensitivity, specificity and accuracy of the outcome for the RBFN test files. The proposed technique has an accuracy rate of 80.95%, with 100% sensitivity and 70.6% specificity in identifying breast cancer. The results are promising as compared to clinical examination by experienced radiologists, which has an accuracy rate of approximately 60–70%. To sum up, technological advances in the field of infrared thermography over the last 20 years warrant a re-evaluation of the use of high-resolution digital thermographic camera systems in the diagnosis and management of breast cancer. Thermography seeks to identify the presence of a tumour by the elevated temperature associated with increase blood flow and cellular activity. Of particular interest would be investigation in younger women and men, for whom mammography is either unsuitable or of limited effectiveness. The paper evaluated the high-definition digital infrared thermographic technology and knowledge base; and supports the development of future diagnostic and therapeutic services in breast cancer imaging. Through the use of integrative ANN and bio-statistical methods, advances are made in thermography application with regard to achieving a higher level of consistency. For breast cancer care, it has become possible to use thermography as a powerful adjunct and biomarker tool, together with mammography for diagnosis purposes.

Keywords: Breast cancer; Early detection; Artificial neural network; Receiver operating characteristics; Bio-statistical methods; Integrative thermogram

*Corresponding author. Email: myknng@ntu.edu.sg

Journal of Medical Engineering & Technology
ISSN 0309-1902 print/ISSN 1464-522X online © 2008 Informa UK Ltd.
http://www.tandf.co.uk/journals
DOI: 10.1080/03091900600562040

1. Introduction

Breast cancer is one of the most common malignancies among women in the world today [1]. It constitutes 18% of cancer among women and this figure is increasing every year. In Singapore, the figure stands at 20% [2]. Each year, more than 1000 women are diagnosed with breast cancer and the age group with the highest incidence is the 50s to 60s age group.

Breast cancer is caused by the epithelial cells, which are found along the terminal duct lobular unit [1]. In general, breast cancer can be categorized as invasive or non-invasive based on their characteristic pattern. Abnormal growth of epithelial cells can lead to the formation of a tumour [3]. If the growth is restricted, the cancer is classified as benign. If the growth is rapid or has the ability to progress to other regions of the body, it is classified as malignant or carcinoma. More often than not, a malignant breast is firm and irregular in shape. However, confirmation can only be made after mammography and clinical examination (biopsy).

Currently, there are many methods available for breast cancer detection, although detection can be difficult. Figure 1 summarizes these methods, which are based on the underlying principles of wave theory, heat energy, audio/magnetic field and electric properties. At present, mammography is the gold standard for breast cancer detection. The other methods mainly play complementary roles by providing additional critical data for breasts unsuitable or difficult to analyse using X-rays [4].

Thermography is a non-invasive screening method that is economical, quick and does not inflict any pain on the patient. It is a relatively straightforward imaging method, widely used in the medical arena, that detects the temperature variation on the surface of human skin. Thermography is complimentary to other techniques; as it is a test of physiology it alone is not sufficient for medical practitioners to make a diagnosis. However, when used adjunctively with other laboratory and outcome assessment tools, such as anatomical techniques including mammography, ultrasound and computed tomography (CT) scanning, thermography may contribute to the best possible evaluation of breast health. In this paper, an integrative bio-statistical method comprising regression, receiver operating characteristics (ROC) and artificial neural networks (ANNs) is used to analyse the thermograms.

Thermography for breast cancer detection involves applying a thermal imager to detect and record the heat pattern of the breast surface. The underlying principle of this approach is that if there is a tumour beneath the breast, it will use more nutrients to supplement its growth (with angiogenesis). As a result of this increase in metabolism rate, the temperature of the tumour site will tend to increase through heat transfer from the tumour in all directions. Therefore the tumour is not seen as a precise localized hot spot, but as a diffused area on the breast surface [5].

Breast thermography holds great potential for early detection of breast lumps. It has been reported that it can

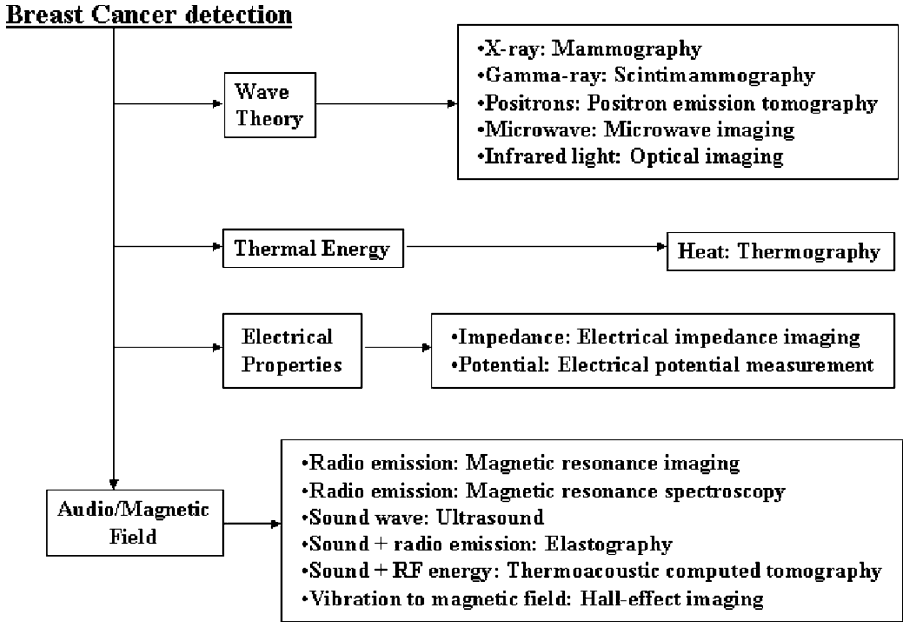

Figure 1. Methods for breast cancer detection.

detect breast cancer 10 years earlier than the traditional method—mammography [1]. Although research and investigation into the application of thermography in breast cancer detection has been ongoing for the last three decades, the results have not been consistent so far. Clinical examination has an accuracy rate of about 70% [2]. It is desired that thermography should equal or exceed this accuracy rate, and have high sensitivity and specificity. However, due to inconsistencies in diagnosis from breast cancer thermograms, it is not yet used in Singapore as an adjunct tool to mammography. This work thus seeks to achieve an improved and reliable level of consistency in the use of breast cancer thermography by virtue of a novel and unique approach encompassing bio-statistical methods and ANN.

More specifically, the use of the radial basis function network (RBFN) [6] will be the main focus. Neural networks (NN) are pattern recognition programs that have the ability to predict outcomes based on various inputs fed into the program. Hence, they can predict whether the breast is healthy or cancerous. Linear regression is incorporated to increase the accuracy of the results by selecting only useful and relevant inputs.

2. Image analysis tools

2.1. Thermography

Infrared (IR) thermography was originally developed for military purposes. In recent times, its uses have extended to engineering applications and medical imaging. IR thermography makes use of a thermal imager to detect the IR radiation and measure the heat pattern of the object surface or human skin [7–9]. It is passive in nature, so it will not emit any harmful radiation or subject the patient to any risk. Hence, many considered it to be a physiological test, compared to anatomical tests such as computed tomography (CT) imaging or X-rays. In addition, it is a non-contact screening process, making it a hygienic procedure. Other advantages of thermography include high portability and real time imaging, which made it possible for the data to be recorded in computers for processing.

The imager converts the thermal energy to electrical signals in order to display the temperature profile of the subject, which contains a number of colours indicating different temperatures. The thermal imager should be used in an indoor environment where external factors, such as ambient temperature, humidity and electrical sources, can be controlled.

Figure 2 shows a basic thermal imager set up. The target distance between the imager and the target is usually between 0.5 m and 6 m. The selected distance should optimize the resolution of the colour display of heat patterns. The ideal ambient condition is between 20°C to 25°C. As for relative humidity, it should range between 40% and 60%.

2.2. Artificial neural networks

Artificial neural networks (ANNs) are one of the burgeoning areas of current research and attract people from a wide variety of disciplines of science and technology. It is known that the human brain is built of cells called neurons. A collection of neurons can perform separate functions simultaneously, and is called a neural network [10]. In ANNs, the fundamental unit that we employ is an approximated electronic/mathematical model of a neuron. The connection strength between layers is called weight. The process of adjustment of weights is called learning or training. Humans are intelligent because evolution has equipped them with a variety of functions that enable them to learn. The learning procedure constructs new representations, and the results of learning can be viewed as numerical solutions to the problem of whether to use local or distributed representations. Basically there are three types of learning: supervised learning (training with teacher), unsupervised learning (training without teacher) and hybrid learning (which falls between supervised and unsupervised learning).

2.2.1. Backpropagation network (BPN). The backpropagation algorithm (BPA) is an iterative gradient algorithm designed to minimize the mean square error between the actual output and the desired output. This algorithm is also known as the generalized delta rule [10]. The neurons in layers other than the input and output layers are called hidden units or hidden nodes, as their outputs do not directly interact with the environment. With the BPA, the weights associated with the hidden layers can also be adjusted and thus enable the ANN to learn. For our study we tried with both single layer perceptron (SLP) and multilayer perceptron (MLP), but the performance was better with SLP. In the following section we have discussed the workings of the NN.

If the class boundaries are more complex, a MLP feedforward NN with sigmoid activation function is more suitable [11]. In its simplest feedforward form, an NN is a collection of connected activatable units (neurons), wherein the connections are real value weights. The network is presented with an activation pattern on its input units, i.e. a set of features of images to be classified. Activation spreads in the forward direction from the input units to output units through between layers (hidden layer) over the weighted connections. Typically, the activation coming into a unit from other units is multiplied by the weights on the links over which it spreads, only in forward direction in the case of feedforward networks (in both directions in the case of recurrent or feedback networks), and then is added together with other incoming activation. The result is

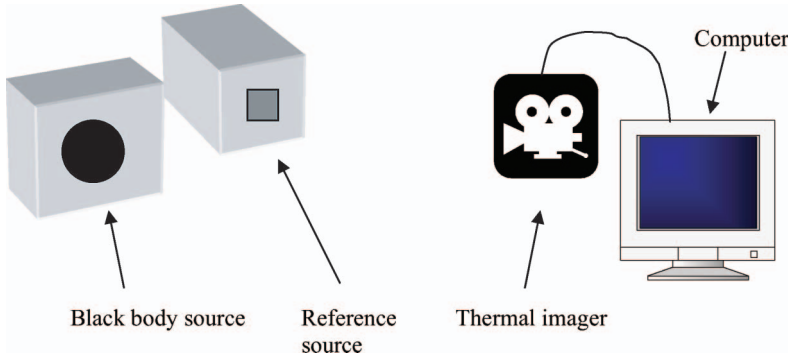

Figure 2. Thermal imager setup.

thresholded (i.e. the unit 'turns on' if the resulting activation is above the units threshold). This process is meant to roughly mimic the way in which activation spreads through the networks of neurons in the brain.

After activation has spread through a feedfoward network, the resulting activation pattern on the output units encodes the network's answer to the input. In most applications, the network learns a correct mapping between input and output patterns via a learning algorithm. Typically the weights are initially set to small random values. Then a set of training inputs is presented sequentially to the network. In the backpropagation learning procedure, after each input has propagated through the network, weights are adjusted to reduce the difference between the network's output and the correct output. In the present case, a learning constant, $\eta = 0.9$, which controls the step size, is chosen by trial and error. Each iteration is called a training cycle and a complete pass of training cycles through the set of training inputs is called a training epoch. This type of procedure is known as supervised learning, since a teacher supervises the learning by providing correct output values to guide the learning process. In contrast, in unsupervised learning there is no teacher, and the learning system must learn on its own using less detailed environmental feedback on its performance.

2.2.2. Radial basis function network (RBFN). RBFN is a kind of feedforward and unsupervised learning paradigm. A simple RBFN consists of three separate layers: the input, hidden and output layers. The first part of the training cycles involves clustering of input neurons. Mathematically, the clustering is done using the dynamic K-means algorithm [10]. At the end of the clustering process, the radius of the Gaussian functions at the middle of the clusters will be equivalent to the distance between the two nearest cluster centres.

During the training, the RBFN is required to fulfil two tasks: firstly, to determine the middle of each hypersphere, and secondly, to obtain its radius. The first task is carried out by allocating the weights of the processing elements (PEs). This can be achieved by using an unsupervised clustering algorithm. It is important to note that the output neuron in the prototypical layer of a RBFN is in a function of the Euclidean distance. This distance is measured from the input neuron to the weighted neuron. The unsupervised learning phase in the hidden layer of RBFN is followed by another different supervised learning phase. This is the stage where the output neurons will be trained to associate each individual cluster with their own distinct shapes and sizes. Normally, the training speed of RBFN is faster than BPN, and it has the ability to detect data that are not within the norm and thus can make better decisions during classification problems. Nevertheless, the first few thousand training cycles of RBFN are unsupervised and, as a result, important information could be overlooked. The bounded transfer function may hinder the network's ability to solve regression problems and when compared to BP, it is not as effective in providing a compact distributed function.

The input and output neurons of RBFN and perceptron are alike [10]. The major difference lies in the hidden neuron. In most cases, it is governed by the Gaussian function. This is different from other processing neurons that produce an output based on the weighted sum of the inputs. Input neurons of RBFN are not involved in the processing of information, and their sole function is to input the given data to the receiving nodes. Using a linear transfer function, these receiving nodes will decide the weights to be allocated to each PE that follows. They are governed by the following transfer functions:

$$y_i = f_r(r_i) \quad r_i = \sqrt{\sum_{j=1}^{n} (x_j - w_{ij})^2}, \tag{1}$$

where w_{ij} represents the amount of weights allocated to the inputs of the neuron i. f_r represents the Gaussian function, which is the preferred choice of most researchers.

$$f_r(r_i) = exp(-r_i^2/2\sigma_i^2), \tag{2}$$

where σ_i represents the standard deviation of the Gaussian distribution. Every neuron at each hidden layer will have its own unique σ_i value.

2.3. Bio-statistical methods

2.3.1. Linear regression (LR) analysis. Regression analysis, also known as least squares regression, is a statistical technique used to determine the unique curve or line that best fits all the data points. The underlying principle is to minimize the square of the distance of each data point to the line itself. In regression analysis, there are two variables—dependent and independent. The dependent variable is to be estimated or predicted.

The most important result obtained in the analysis is the coefficient of determination, R^2. This is an indication of how tightly or sparsely clustered the data points are and it is a value that lies between 0 and 1. In other words, it is a measure of the correlation between the two variables. Correlation refers to the predictability of the change in the dependent variable given a change in the independent variable.

LR uses a straight line to fit the data points (figures 3 and 4). It is a simple yet effective way to obtain the correlation between two variables. However, a few assumptions are made in using LR. Firstly, a linear relationship is assumed between the two variables, and this might not always be the case. Secondly, the dependent variable is assumed to be normally distributed with the same variance as its corresponding value of independent variable. Mathematically, LR model is given by $Y = Ax + B$.

2.3.2. Receiver operating characteristics (ROC) curves. ROC curves are used to assess the diagnostic performance of a medical test to discriminate unhealthy cases from healthy cases [12]. Very often in a medical test, perfect separation between unhealthy and healthy cases is not possible if the discrimination is based on a threshold value. Figure 5 illustrates this phenomenon. The threshold value, γ, is shown in the figure. The majority of those without the disease will be correctly diagnosed as healthy (TN). Similarly, the majority of those with the disease will be correctly diagnosed as unhealthy (TP). However, there will also be one group of diseased patients wrongly diagnosed as healthy (FN) and one group of healthy patient wrongly diagnosed as unhealthy (FP). Table 1 summarizes all the possibilities, TN, TP, FN and FP, and their respective algebraic representation. With that, four important criteria can be defined—sensitivity, specificity, positive predictive value (PPV) and negative predictive value (NPV)—and they are commonly used in ROC analysis to assess the

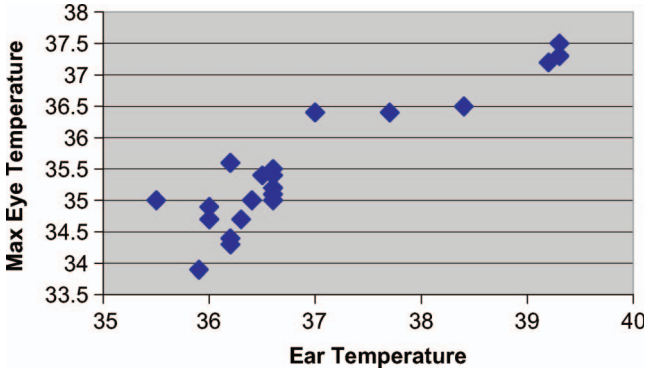

Figure 3. A scatter plot of maximum eye versus ear temperature.

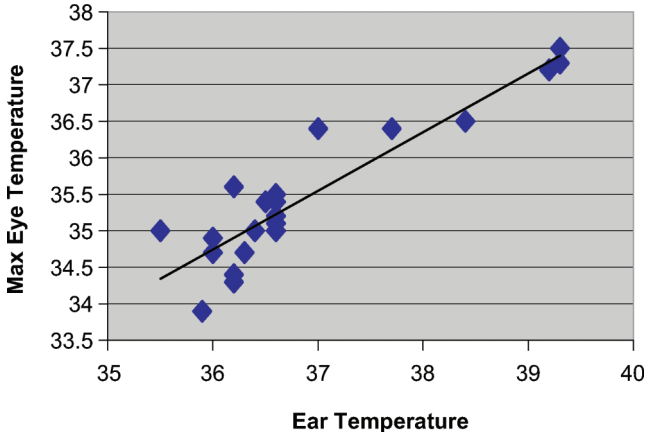

Figure 4. A regression line fitted to the scatter data of Figure 3.

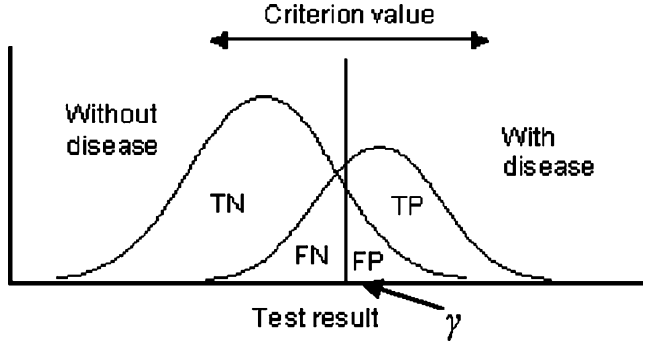

Figure 5. A typical discrimination curve for ROC analysis.

Table 1. Basic mathematical formulae for ROC analysis.

Test	Disease	Number	Disease	Number	Total
Result	Present	n	Absent	m	
Positive	True positive (TP)	a	False positive (FP)	c	$a+c$
Negative	False negative (FN)	b	True negative (TN)	d	$b+d$
Total		$a+b$		$c+d$	

credibility of the test. The mathematical formulae are summarized as:

- Sensitivity: the probability that test is positive in the unhealthy population $= a/(a+b)$
- Specificity: the probability that the test is negative in the healthy population $= d/(c+d)$
- PPV: given a positive forecast, the probability that it is correct = sensitivity/(1 – specificity)
- NPV: given a negative forecast, the probability that it is correct = (1 – sensitivity)/specificity

In the ROC curves analysis result, both sensitivity and specificity are displayed for all criteria. This allows the user to choose the optimum criterion, which ought to have high values for both sensitivity and specificity. The value of sensitivity is inversely proportional to that of specificity. This can be easily illustrated by the threshold value γ. A low γ will ensure that those with the disease will be detected. But this will also cause those without the disease to be classified as diseased. On the other hand, a high γ will allow the healthy group to be correctly categorized but will miss out on the diseased group.

Figure 6 shows an example of the ROC curves. The vertical axis is the sensitivity while the horizontal axis shows the (100 – specificity). This once again reinforces the fact that there is a trade-off between sensitivity and specificity.

The area under the ROC curve is important information obtained in the analysis. The value lies between 0.5 and 1. A value of 0.5 implies that the test cannot discriminate the unhealthy group from the healthy group, whereas a value of 1 implies that the test can distinguish the two groups perfectly.

3. Data acquisition

The breast cancer data were collected from the Department of Radiology Diagnostics, Singapore General hospital [13,14], where 90 breast thermography patients were chosen at random. It was ensured that patients were within the recommended period of the 5th to the 12th and 21st days after the onset of menstrual cycle, since vascularization is at basal level with least engorgement of blood vessels [13]. The accuracy of thermography in women whose thermal images are taken in a suitable period is higher (80%) than the total population of patients (73%). For the analysis here, thermograms of eight patients were excluded for analysis as seven of the patients had history of mastectomy and one patient had a highly distorted breast on one side. Thus, thermograms of 82 patients were used in the analysis: 30 asymptomatic patients (age = 51 ± 8), 48 patients (age = 46 ± 10) with benign breast abnormality on either side of the breasts, and four patients (age = 45 ± 5) with cancer on either side of the breasts.

The thermal imager used was Avio TVS-2000 MkII ST (Tokyo, Japan) [15], which possesses a wide range of capabilities, including image enhancement, freeze-frame mode, automated tracking of heat pattern and recording. The venue was an indoor environment where the room temperature was between 20°C and 22°C (within ± 0.1°C) and the humidity was about 60% ± 5%. Heat sources such as sunlight or other electrical appliances were reduced to a minimum due to their effect on the ambient temperature. Prior to the screening, the patients were instructed to abstain from alcohol, cigarettes and any form of drugs that would affect the body's biological system, which would result in a change in body temperature. In addition, the patient's breast surface should be free from powder or ointments.

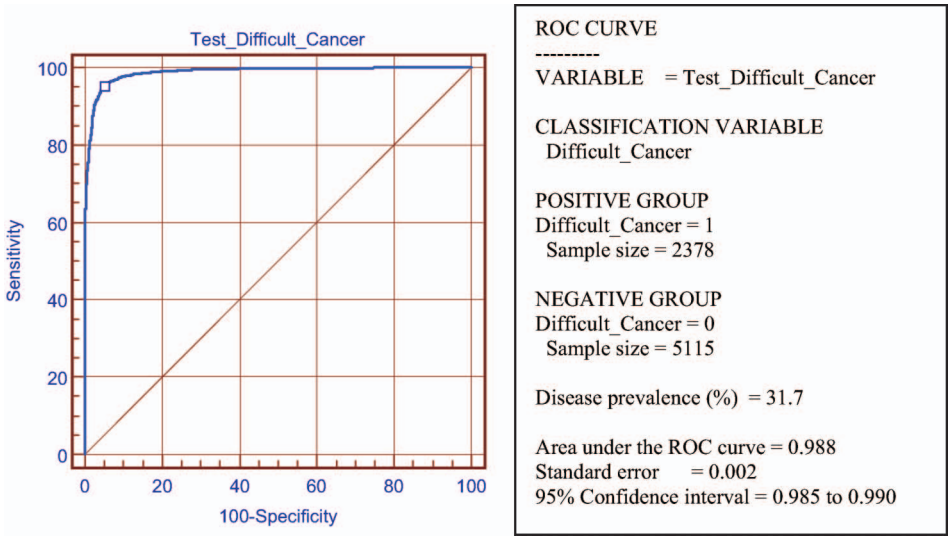

Figure 6. A typical ROC curve.

3.1. Procedures for thermal imaging

The patients were required to abstain from any physical activities for 20 minutes before the start of thermal screening [13]. This is to reduce the body's metabolism rate so as to allow the overall body temperature to stabilize. During the thermographic examination, the patients were required to remove clothing from their upper bodies and their hands were positioned behind their heads. During the imaging, three thermograms are taken: one frontal image and two lateral images. Each image was then improved digitally to enhance the resolution.

Figures 7 and 8 show two typical examples of thermograms—healthy and cancerous. In the healthy state, an individual's breasts are generally symmetrical, although they may differ slightly in size, and the breast outline as portrayed by the thermogram is smooth and regular with a convex contour. The thermal image and quantitative levels of heat are usually similar, but never identical in the two breasts. The background upon which the breast is superimposed is cool compared with the upper thorax and the infra-mammary fold, and the nipple itself stands out as a round cool spot, frequently outlined by a faintly warmer zone. The distinguishing hallmark of abnormality (cancerous) however is vascular discrepancy encompassing:

a) differences in the number and calibre of veins and their quantitative thermal measurements;
b) focal areas of heat, whether periareolar or localised elsewhere, and not necessarily identified with a particular vein; and
c) a diffuse increase in background temperature occasionally associated with breast enlargement. An additional abnormality is the loss of the regular convex contour of the breast outline referred to as the 'edge sign'.

Temperature data are extracted from the breast thermograms. The thermograms consist of many coloured pixels, each representing a temperature. From the thermograms alone, it is possible for an experienced medical practitioner to diagnose abnormalities such as a cyst. After the temperature of every pixel is compiled, bio-statistical technique can be used to analyse them, for example by determining the mean, median and modal temperature of the breast region.

4. Integrated approach

The proposed advanced approach is a multi-pronged method comprising LR, RBFN, and ROC analysis. It is a novel and powerful integrated technique that can be used to analyze complicated and large measured data.

4.1. Step 1: linear regression (LR)

LR reflects the correlation between the variables and the actual health status (healthy or cancerous) of the subject, which is decided by mammography and biopsy. Hence, LR is used to decide if a particular variable should be used for inputs in the train file. A variable will be used as input in the NN if and only if it has a strong correlation with the outcome (health status of the patient).

The following data was compiled and collected from each subject [13,14]:

- **Temperature data from thermograms:**
  - mean temperature of left breast;
  - mean temperature of right breast;
  - median temperature of left breast;
  - median temperature of right breast;
  - modal temperature of left breast; and
  - modal temperature of right breast.

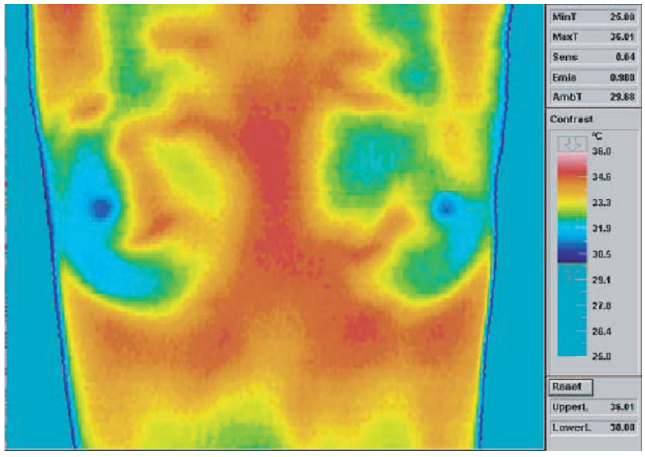

Figure 7. Symmetrical thermogram of a healthy 24-year-old female.

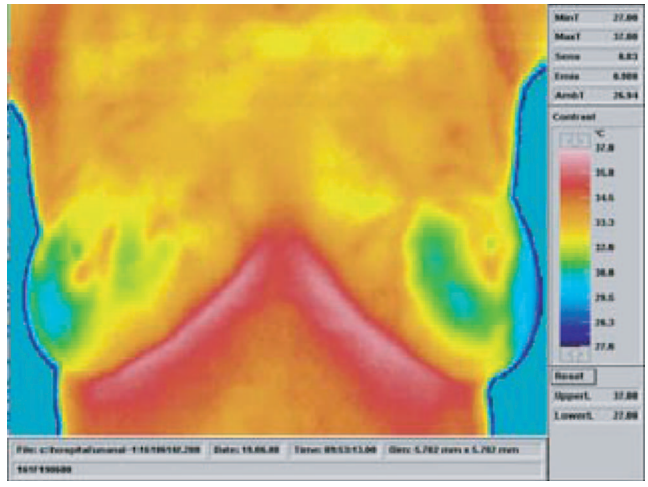

Figure 8. Cancerous thermogram of a 50-year-old female (invasive lobular Ca grade I in left lateral breast).

- **Biodata from questionnaire:**
  - age of patient;
  - family history of breast cancer;
  - hormone replacement therapy;
  - age of menarche patient;
  - presence of palpable lump;
  - previous breast surgery/biopsy;
  - presence of nipple discharge;
  - pain in the breast;
  - menopause at the age of >50 years old; and
  - first child at the age of >30 years old.

4.2. Step 2: ANN RBFN

Based on the various inputs fed into the network, RBFN is trained to produce the desired outcome, which is either positive (1) for cancer and benign cases or negative (0) for healthy cases. Different combinations of learn rule, transfer rule and options will be tested under the wide umbrella of RBFN. When this is done, the RBFN algorithm possesses the ability to predict the outcome when there are new input variables. The advantages of using RBFN include fast training, superior classification and decision-making abilities as compared to other networks such as BP. For this breast cancer study, conventional BP training [14] and testing are also included and the results are compared with that of RBFN.

4.3. Step 3: ROC analysis

Next, ROC is used to evaluate the accuracy, sensitivity and specificity of the outcome of RBFN test files to check if the RBFN is well built or not.

4.4. Flow chart of the proposed method

The software needed for all processes includes:

- Image J: to view thermograms from thermal imager and extract temperature data;
- MS Excel Statistical Toolbox: to normalize raw temperature data and perform statistical analysis (e.g. mean, median, standard deviation);
- MedCal: to determine the correlation of each variable with the output (health status);
- NeuralWorks Pro II: for training and testing of data & building an algorithm for the data; and
- MedCal: to evaluate the effectiveness of the computed method.

Figure 9 shows the entire process in a flow chart, including the steps prior to advanced integrated technique (AIT). For AIT, either RBFN or BPN can be used.

5. Results and discussion

5.1. Summarized results for step 1

In general, the coefficient of determination, shown in table 2, is low for both the temperature related data and the

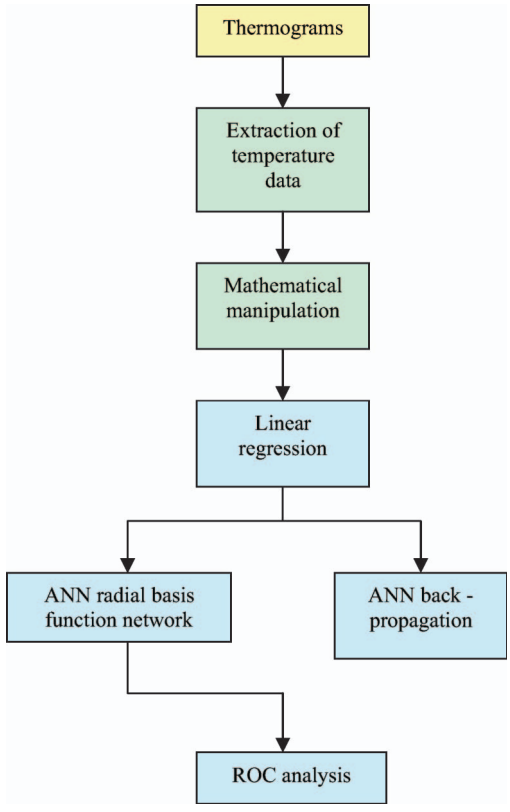

Figure 9. Flow chart showing the advanced integrated technique for BC thermograms.

Table 2. Summarized results for linear regression.

No.	Independent X	Coefficient of determination
1	Mean temperature of left breast	0.03412
2	Median temperature of left breast	0.03110
3	Mode temperature of left breast	0.02850
4	Mean temperature of right breast	0.04740
5	Median temperature of right breast	0.04520
6	Mode temperature of right breast	0.04900
7	Age of patient	0.00430
8	Family history	0.00500
9	Hormone replacement therapy	0.27313
10	Age of menarche of patient	0.04740
11	Presence of lump	0.05190
12	Previous breast surgery/biopsy	0.02650
13	Presence of nipple discharge	0.00830
14	Pain in the breast	0.02500
15	Menopause at more than 50 years of age	0.02500
16	First child at more than 30 years of age	0.00650

biodata, since the relationship between the variables and the health status (healthy or unhealthy) is not obvious. However, it is noted that the coefficient of determination for the temperature related data is generally higher than that of the biodata. This reinforces the fact that thermography can be used as an adjunct tool as there suggests a strong correlation between the surface temperature of the breast and the health status of the patient. The variables with the highest and lowest coefficients of determination are the modal temperature of the right breast and the 'first child at more than 30 years old' criterion. The percentage of score is obtained from the number of correct predictions over the total number of cases made by the ANN. Tables 3 and 4 summarize the various combinations of learn rule, transfer rule and options that were tested.

Table 3. Selected results for RBFN and BP SLP with selected and various combination of learn and transfer rules (with various options tested).

ANN type	Learn rule	Transfer rule	Option	Score (%)
RBFN	Delta rule	DNNA	–	80.95
	Norm-cum-delta	DNNA	–	80.95
	Ext DBD	DNNA	–	80.95
	QuickProp	Linear	–	80.95
	Delta bar delta	TanH	–	80.95
	Delta rule	DNNA	Connect Prior	80.95
	Delta rule	DNNA	Linear O/P	80.95
	Delta rule	DNNA	Softmax O/P	80.95
	Delta rule	DNNA	Connect Bias	80.95
	Delta rule	DNNA	MinMax Table	80.95
	Norm-cum-delta	DNNA	Connect Prior	80.95
	Norm-cum-delta	DNNA	Linear O/P	80.95
	Norm-cum-delta	DNNA	Softmax O/P	80.95
	Norm-cum-delta	DNNA	Connect Bias	80.95
	Norm-cum-delta	DNNA	MinMax Table	80.95
	Ext DBD	DNNA	Connect Prior	80.95
	Ext DBD	DNNA	Linear O/P	80.95
	Ext DBD	DNNA	Softmax O/P	80.95
	Ext DBD	DNNA	Connect Bias	80.95
	Ext DBD	DNNA	MinMax Table	80.95
	QuickProp	Linear	Connect Prior	80.95
	QuickProp	Linear	Linear O/P	80.95
	QuickProp	Linear	MinMax Table	80.95
	Delta bar delta	TanH	Connect Prior	80.95
BP	Ext DBD	TanH	–	80.95
	Delta bar delta	Linear	–	80.95
	Delta bar delta	Sigmoid	–	80.95
	Delta bar delta	Sigmoid	Fast Learning	80.95
	Delta bar delta	Sigmoid	Minimal Confg	80.95
	Delta bar delta	Sigmoid	Bipolar I/P	80.95

5.2. Selected results for step 2

The highest level of accuracy attained by both ANN RBFN and BP is 80.95%. However, as many as 37 RBFN have achieved 80.95%, whereas only nine BPNs manage to achieve this score. Hence, the RBFN is superior and credible to BP in the prediction of the breast cancer, since data is rather complicated and large with 10 input variables (selected from LR).

5.3. Selected results (with area >0.85) for step 3

The accuracy rate in step 2 is only based on the number of correct predictions. However, it does not take into account the percentage of correct predictions of the positive cases or the percentage of correct predictions of the negative cases. Hence there is a need for ROC analysis on the selected RBFN with high accuracy rate, in order to further verify its effectiveness.

Evaluating the RBFN with ROC (tables 4 and 5) shows that the NN model is well built. The area under curve for most RBFN is higher than 0.85. These RBFNs also

Table 4. Selected results for RBFN and BP MLP with selected combination of learn rule, transfer rule and options, tested with different hidden neurons.

ANN Type	Learn rule	Transfer rule	Option	Hidden neurons	Score (%)
RBFN	Delta rule	DNNA	Connect Prior	0	80.95
	Delta rule	DNNA	Connect Prior	2	80.95
	Delta rule	DNNA	Connect Prior	3	80.95
	Delta rule	DNNA	Connect Prior	4	80.95
	Norm-cum-delta	DNNA	Linear O/P	0	80.95
	Norm-cum-delta	DNNA	Linear O/P	4	80.95
	Norm-cum-delta	DNNA	Linear O/P	5	80.95
	Ext DBD	DNNA	Softmax O/P	0	80.95
	Ext DBD	DNNA	Softmax O/P	3	80.95
	Ext DBD	DNNA	Softmax O/P	4	80.95
	Ext DBD	DNNA	Softmax O/P	5	80.95
	QuickProp	Linear	Connect Bias	3	80.95
	QuickProp	Linear	Connect Bias	5	80.95
BP	Delta bar delta	Sigmoid	Fast Learning	0	80.95
	Delta bar delta	Sigmoid	Minimal Confg	0	80.95
	Delta bar delta	Sigmoid	Bipolar I/P	0	80.95

Table 5. Selected results for ROC analysis for RBFN SLP with selected and various combination of learn rule and transfer rule (with various options tested).

Learn rule	Transfer rule	Option	Area under curve	Sensitivity	specificity
Delta bar delta	TanH	–	0.888	75	94.1
Delta bar delta	TanH	Connect prior	0.888	75	94.1
Delta bar delta	TanH	Connect bias	0.899	81.2	94.1

Table 6. Selected results ROC analysis for ANN RBFN MLP with selected combination of learn rule, transfer rule and options, tested with different hidden neurons.

Learn rule	Transfer rule	Option	Hidden neuron	Area under curve	Sensitivity	Specificity
Delta rule	DNNA	Connect prior	1	0.866	78.1	94.1
QuickProp	Linear	Connect bias	1	0.869	75	82.4
QuickProp	Linear	Connect bias	3	0.858	75	88.2
QuickProp	Linear	Connect bias	4	0.869	78.1	82.4
Delta bar delta	TanH	Connect prior	0	0.899	81.2	84.1
Delta bar delta	TanH	Connect prior	2	0.877	84.4	76.5
Delta bar delta	TanH	Connect prior	4	0.914	65.6	100
Delta bar delta	TanH	Connect prior	5	0.89	81.2	88.2

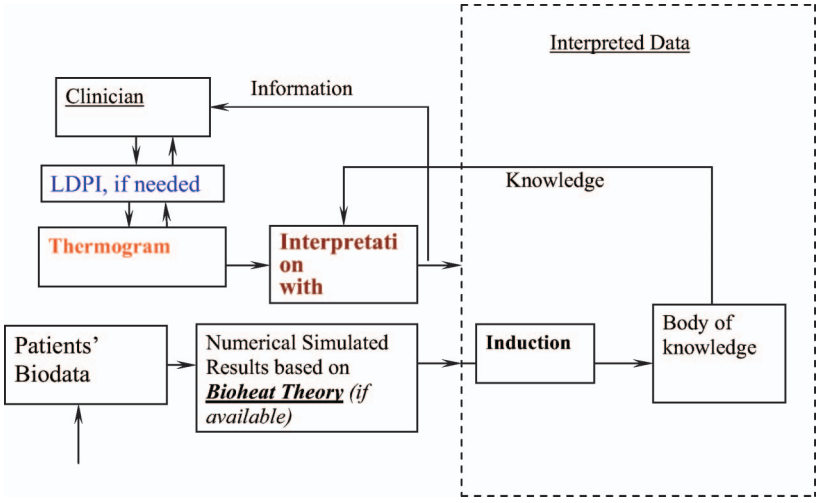

Figure 10: Outline of a clinical protocol with the use of multi-modality environment including simulation, patient biodata, LDPI and the interpretation of thermograms.

achieved high sensitivities (>75%) and high specificities (about 90%). This indicates that the overall diagnostic performance is competitive with that of mammography. The best performing RBFN is a multi-layered perceptron (MLP, table 6) with delta bar delta as the learn rule, TanH as the transfer rule and connect prior as the selected option. The number of hidden neurons is 5 and the ROC area achieves 0.89. Although its area under curve is not the highest, it possesses very high sensitivity (81.2%) and high specificity (88.2%). In brief, the NNs with delta bar delta as the learn rule outperformed other learn rules.

Ultimately, the proposed AIT analysis should be integrated for clinical application. Figure 10 outlines a possible clinical protocol with the use of multi-modality approaches including numerical simulation [16–18], patient biodata, laser Doppler perfusion imaging (LDPI) [19] and the data interpretation of thermograms. To overcome a manual data analysis that is highly inefficient and prone to human error, a computer-aided tool to assist the specialist in the analysis of thermograms is desirable [20]. Figure 11 further shows the framework of the proposed system for analysis of the thermograms. The system relies on the current thermogram approach along with a database supplying clinical test results, patient records, physiological data, historical thermo-images, genetic information, etc, to analyse automatically the

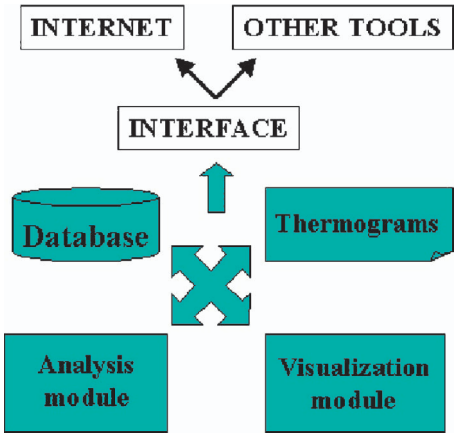

Figure 11. Framework for the computer-aided analysis of thermograms.

likelihood of breast cancer development. The analysis module has been discussed in §4. In addition to analysis, the system should allow for the 3D reconstruction of suspected tumour development based on the heat patterns associated with the thermograms. This visualization module would enable the specialist to have a good picture of the location, size and topology of the suspected tumour. The information would be useful, as further tests could then be conducted to search for tumour development in that area. One of the possible documented visualization modules is the thermal texture mapping algorithm (TTM) [21,22].

6. Conclusion & future work

Thermography measurements allow changes in tumour angiogenesis to be evaluated and may assist in dynamic monitoring of therapy. However, their full potential has yet to be realised. A major challenge is to change the perceptions of clinical and insurance professionals, so that thermographic evaluation is more accepted. Through the use of ANN and bio-statistical methods, progress has been made in thermography application, and a higher level of consistency has been achieved. This has been made possible with the introduction of the novel AIT in thermogram analysis.

To conclude, this paper has investigated the diagnostic potential of infrared thermography in light of recent technological advances, utilizing existing advanced thermographic equipment and applying the multidisciplinary experience in data analysis to breast care. Importantly, the work does not seek to replace or provide an alternative to existing mainstays of screening (clinical examination and mammography), but to provide a scientifically valid adjunct to existing breast cancer services.

The next focus in research on breast cancer detection using thermography would be the attempt to pinpoint the actual location and size of the tumour (such as by TTM) if the diagnosis is positive. This would then definitely be a major step forward in the fight against breast cancer.

Acknowledgements

The first author would like to thank Dr Ng F.C. and Dr Sim L.S.J., Senior Consultant Radiologists, Department of Diagnostic Radiology of the Singapore General Hospital, Singapore on their interpretation of post-surgery vessel phenomena and complications, etc.

References

[1] Dixon, M., 1999, *ABC of breast diseases* (Edinburgh, UK: BMJ Publishing Group).
[2] Breast Cancer Foundation, http://www.bcf.org.sg/ (accessed 18 December 2005).
[3] Hirshaut, Y. and Pressman, P., 1996, *Breast cancer. The complete guide* (New York, USA: Bantam Trade).
[4] Fok, S.C., Ng, E.Y.-K. and Thimm, G.L., 2003, Developing case-based reasoning for discovery of breast cancer. *Journal of Mechanics in Medicine and Biology*, **3,** 231–246.
[5] Ng, E.Y.-K. and Sudharsan, N.M., 2001, Effect of blood flow, tumour and cold stress in a female breast: a novel time-accurate computer simulation. *International Journal of Engineering in Medicine*, **215,** 393–404.
[6] Battelle, http://www.battelle.org/pipetechnology/ (last accessed 18 December 2005).
[7] Ng, E.Y.-K., 2005, Is thermal scanner losing its bite in mass screening of fever due to SARS? *Medical Physics*, **32,** 93–97.
[8] Ng, E.Y.-K. and Kaw, G.J.L., 2005, IR scanners as fever monitoring devices: physics, physiology and clinical accuracy. In N. Diakides (Ed.) *Biomedical Engineering Handbook* (Florida, USA: CRC Press), Chapter 24: pp. 1–24.
[9] Ng, E.Y.-K. and Kee, E.C., 2005, Fever mass screening tool for infectious diseases outbreak: integrated artificial intelligence with bio-statistical approach in thermogram analysis. In F. Columbus (Ed.) *Progress in Avian Influenza Research* (NY, USA: Nova Science Publishers), pp. 1–24.
[10] Hopgood, A., 2000, Intelligent systems for engineers and scientists. Library of Congress Cataloging in Publication Data.
[11] Stamatios, V.K., 2000, *Understanding Neural Networks and Fuzzy Logic-Basic Concepts and Applications* (Chennai, India: Prentice Hall).
[12] Receiver Operating Characteristics (ROC), http://www.medcalc.be/ (accessed 18 December 2005).
[13] Ng, E.Y.-K., Ung, L.N., Ng, F.C. and Sim, L.S.J., 2001, Statistical analysis of healthy and malignant breast thermography. *International Journal of Medical Engineering & Technology*, **25,** 253–263.
[14] Ng, E.Y.-K., Fok, S.C., Peh, Y.C., Ng, F.C. and Sim, L.S.J., 2002, Computerized detection of breast cancer with artificial intelligence and thermograms. *International Journal of Medical Engineering & Technology*, **26,** 152–157.
[15] Fok, S.C., Ng, E.Y.-K. and Tai, K., 2002, Early detection and visualization of breast tumor with thermogram and neural network. *Journal of Mechanics in Medicine and Biology*, **2,** 185–196.
[16] Ng, E.Y.-K. and Sudharsan, N.M., 2000, Can numerical simulation adjunct to thermography be an early detection tool? *Journal of Thermology International*, **10,** 119–127.
[17] Ng, E.Y.-K. and Sudharsan, N.M., 2001, Numerical computation as a tool to aid thermographic interpretation. *International Journal of Medical Engineering & Technology*, **25,** 53–60.
[18] Ng, E.Y.-K. and Sudharsan, N.M., 2004, Numerical modelling in conjunction with thermography as an adjunct tool for breast tumour detection. *BMC Cancer*, **4,** 1–26.

[19] Seifalian, A.M., Chaloupka, K. and Parbhoo, S.P., 1995, Laser Doppler perfusion imaging—a new technique for measuring breast skin blood flow. *International Journal of Microcirculation*, **15,** 125–130.

[20] Ng, E.Y.-K. and Fok, S.C., 2003, A framework for early discovery of breast tumor using thermography with artificial neural network. *The Breast Journal*, **9,** 341–343.

[21] Wang, B. and Wang, Y.L., 2003, TTM analysis of 221 cases of microcirculation depression. *Proceedings of the 1st Conference of Thermal Texture Mapping (TTM) Tech. in Medicine and Engineering*, 20–22 October 2003, Houston, Texas, pp. 105–107.

[22] Qi, H., Liu, Z.Q. and Wang, C., 2002, Breast cancer identification through shape analysis in thermal texture maps. *Annual International Conference of the IEEE Engineering in Medicine and Biology Proceedings*, **2,** 1129–1130.